The Interaction of Two Internal Waves with the Mean Flow: Implications for the Theory of the Quasi-Biennial Oscillation

R. A. PLUMB[1]

CSIRO Division of Atmospheric Physics, Aspendale, Victoria, Australia

(Manuscript received 24 May 1977, in revised form 30 August 1977)

ABSTRACT

Internal waves propagating through a dissipative fluid interact with the mean flow. In response to forcing by a single wave, the mean flow evolves to a steady solution. In the presence of two (or more) waves such a solution exists but is unstable. The underlying dynamics in the latter case are basically those discussed by Holton and Lindzen (1972) in their theory of the quasi-biennial oscillation. If viscosity is small but nonzero the zonal flow exhibits a long-period oscillation.

This study elucidates the dependence of the period and structure of the oscillation on the imposed parameters, and clarifies the basic dynamics. In particular, the origin of the downward motion of shear zones is discussed in detail following a demonstration (under realistic assumptions) that anomalies in the mean flow structure cannot propagate downward. Thus it is shown that the increase of radiative cooling coefficient with height in the stratosphere is not crucial to the mechanism while the mesospheric semi-annual oscillation is irrelevant for practical purposes. It is also argued that momentum diffusion in the lower stratosphere may be of crucial importance in the momentum budget of the oscillation.

1. Introduction

The quasi-biennial oscillation of the zonal wind in the tropical stratosphere has been the subject of considerable study in recent years. The explanation put forward by Holton and Lindzen (1972, hereafter denoted by HL), that the oscillation arises from interaction between the mean flow and large-scale equatorial waves propagating through the stratosphere from below, now appears to be well established, following observationally-based comparisons of mean flow acceleration and wave driving (Wallace and Kousky, 1968; Lindzen and Tsay, 1975). A recent theoretical development has been the demonstration that the fundamental properties of wave-mean flow interaction upon which the HL theory depends[2] are not significantly affected when the subtleties associated with atmospheric rotation and meridional structure are taken into account (Andrews and McIntyre 1976a; Boyd, 1976).

The work described in this paper constitutes an investigation of the purely two-dimensional problem with the aims of clarifying the underlying dynamics and of elucidating the dependence of the basic characteristics of the mean flow oscillation on the various imposed parameters of the system. One particular problem associated with the mechanistic explanation of the phenomenon given in HL is the means by which the phase of the oscillation propagates downward. According to their theory an essential part of the mechanism is the establishment of an easterly or westerly flow regime at high levels, either as a consequence of enhanced wave absorption there or because of the presence of the semi-annual oscillation. It is then envisaged that interaction of the upward propagating waves with the shear layer at the lower edge of this flow zone causes the shear layer to move downward. However, the momentum fluxes associated with upward propagating waves at any level z_0 are influenced only by the velocity structure at and below z_0, and it is shown in Section 2 that the wave-generated acceleration at z_0 is independent of conditions above that level (if diffusion of mean momentum is negligible). Hence any mean flow anomaly introduced at high levels has no effect on the subsequent evolution at lower levels.

The evolution to a steady state of the mean flow driven by a single internal wave is discussed briefly in Section 3. In the simplest case of two waves driven by a standing-wave forcing at a lower boundary, a trivial steady solution exists but is unstable as a result of wave-driven enhancement of low-level mean flow perturbations. The linear stability analysis is presented in Section 4. The downward motion of shear zones is shown to be a consequence of the mean flow evolution at *lower* levels. Viscous cases are also considered, and the role of diffusion as a cause of a long-period oscillation in the solutions obtained is clarified.

[1] On leave from the Meteorological Office, U. K.

[2] In particular, in the absence of damping and forcing, steady waves do not interact with the mean flow.

Brought to you by New York University | Unauthenticated | Downloaded 10/07/21 07:05 PM UTC

The full nonlinear problem is solved by numerical integration in Section 5, and the study is extended to more complex cases in Sections 6 and 7. With this background the HL model is discussed in some detail in Section 8. The paper concludes with a summary of the major results and a discussion of their significance for the quasi-biennial oscillation.

2. Basic equations

The derivation of the relevant mathematical relations governing the wave-mean flow interaction problem has been given by Lindzen (1971), Fels and Lindzen (1974) and Plumb (1975), among others. Consider two-dimensional motion in a Boussinesq fluid with buoyancy frequency N, viscosity ν and thermal dissipation rate μ. The vorticity equation is

$$\frac{\partial}{\partial t}(\nabla^2\psi)+\frac{\partial\sigma}{\partial x}-\nu\nabla^4\psi=J(\psi,\nabla^2\psi), \tag{2.1}$$

where ψ is the streamfunction, σ the buoyancy $(-g\Delta\rho/\rho)$ and $\nabla^2\equiv\partial^2/\partial x^2+\partial^2/\partial z^2$. The buoyancy is governed by

$$\frac{\partial\sigma}{\partial t}-N^2\frac{\partial\psi}{\partial x}+\mu\sigma=J(\psi,\sigma). \tag{2.2}$$

The motion is separated into mean and fluctuating components, e.g.,

$$\psi=\bar{\psi}+\psi',$$

where the overbar denotes a horizontal average and the prime a deviation from that average.

The following assumptions and approximations are made:

(i) Neglect of $J(a',b')-\overline{J(a',b')}$ [the "mean field" approximation (Herring, 1963)]. The justification for this widely used approximation hinges on the fact that the nonlinear wave self-interaction component driving the mean flow [i.e., $\overline{J(a',b')}$] acts coherently over a long time scale, allowing a large response, even to small-amplitude forcing, while the remaining term has a frequency twice that of the basic wave and, in consequence, produces a small response.

(ii) Neglect of viscous dissipation of the wave on the grounds that, for present purposes, it is much less effective than thermal dissipation.

(iii) Changes in the mean flow take place over time scales long compared to the time scales of the wave motion (i.e., the wave period and propagation time through the region in question); terms involving $\partial\bar{u}/\partial t$ are ignored in the wave equation.

(iv) The Richardson number $\mathrm{Ri}=N^2/(\partial\bar{u}/\partial z)^2$ is large.

(v) The dissipation rate μ is small compared with the Doppler-shifted wave frequency.

(vi) The mean state stratification N^2 is unaffected by the waves. This assumption can be shown to derive from assumptions (iv) and (v).

Under these assumptions the fluctuating components of (2.1) and (2.2) yield solutions of the form (the notation is that of Plumb, 1975)

$$\psi_n'=\mathrm{Re}[\tilde{\psi}_n e^{ik_n(x-c_nt)}],$$

where

$$\frac{\partial^2\tilde{\psi}_n}{\partial z^2}+\left\{\frac{N^2[1+i\mu/k_n(\bar{u}-c_n)]}{(\bar{u}-c_n)^2}-k_n^2-\frac{\partial^2\bar{u}/\partial z^2}{(u-c_n)}\right\}\tilde{\psi}_n=0. \tag{2.3}$$

The wave momentum flux is

$$\tilde{F}_n=\overline{u_n'w_n'}=-(ik_n/4)\left(\tilde{\psi}_n\frac{\partial\tilde{\psi}_n^*}{\partial z}-\tilde{\psi}_n^*\frac{\partial\tilde{\psi}_n}{\partial z}\right), \tag{2.4}$$

where the asterisk denotes complex conjugate.

By assumptions (iv) and (v), Eq. (2.3) may be solved by a WKB approximation. Thus the momentum flux is found to be of the form (Plumb, 1975)

$$\tilde{F}_n(z)=\tilde{F}_n(0)\exp\left\{-s\int_0^z\frac{N\mu}{k_n(u-c_n)^2}dz'\right\}, \tag{2.5}$$

where s is the sign of the vertical component of group velocity.

Now because of the nonzero dissipation μ, the momentum flux divergence is nonzero, and the mean flow velocity $\bar{u}$ obeys the equation

$$\frac{\partial\bar{u}}{\partial t}-\nu\frac{\partial^2\bar{u}}{\partial z^2}=-\frac{\partial\tilde{F}}{\partial z}. \tag{2.6}$$

In the presence of more than one wave, the fluxes are added[3] to give

$$\frac{\partial\bar{u}}{\partial t}-\nu\frac{\partial^2\bar{u}}{\partial z^2}=-\sum_n\frac{\partial\tilde{F}_n}{\partial z} \tag{2.7}$$

in the manner of HL. Note that for upward propagating waves, $\mathrm{sgn}[F_n(0)]=\mathrm{sgn}(c_n)$. Therefore, from (2.5) and (2.7) absorption of a wave of positive (negative) phase speed produces a positive (negative) mean flow acceleration.

At this stage, it is convenient to write the equations in dimensionless form. Scaling factors for k, c (and $\bar{u}$),

[3] Thus only the self-interaction of individual waves is included. If there exists a number of waves of equal wavenumber k_n (but different c_n), then additional terms should be included representing mutual interaction. However, the time scale of such forcing is of the order of the wave period, and the response will be small [this is equivalent to assumption (i)].

Brought to you by New York University | Unauthenticated | Downloaded 10/07/21 07:05 PM UTC

N and μ are denoted by a circumflex (so that henceforth, e.g., k replaces $k/\hat{k}$). Further dimensionless quantities are

$$\left.\begin{aligned} F_i(0) &= \tilde{F}_i(0)/\hat{F} \\ \alpha &= N\mu/\hat{N}\hat{\mu} \\ \Lambda &= \nu\hat{N}\hat{\mu}/\hat{k}\hat{c}\hat{F} \end{aligned}\right\}.$$

Then invoking new height and time coordinates

$$\zeta = \frac{\hat{N}\hat{\mu}}{\hat{k}\hat{c}^2}z, \quad \tau = \frac{\hat{N}\hat{\mu}\hat{F}}{\hat{k}\hat{c}^3}t, \tag{2.8}$$

Eqs. (2.5) and (2.7) become

$$F_n(\zeta) = F_n(0)\exp\left[-s\int_0^\zeta g_n(\zeta')d\zeta'\right], \tag{2.9}$$

where

$$g_n(\zeta) = \frac{\alpha}{k_n(\bar{u}-c_n)^2}, \tag{2.10}$$

$$\frac{\partial\bar{u}}{\partial\tau} - \Lambda\frac{\partial^2\bar{u}}{\partial\zeta^2} = -\sum_n \frac{\partial F_n}{\partial\zeta}. \tag{2.11}$$

One observation immediately springs from (2.9)–(2.11). Consider the case of upward propagating waves, $s=+1$. The wave-driven contribution to the mean flow acceleration is $-\partial F_n(\zeta)/\partial\zeta = +g_n(\zeta)F_n(\zeta)$. The flux amplitude from (2.9) is a function only of the flow profile in $\zeta' \leqslant \zeta$ (i.e., the region through which the wave has propagated), while the local attenuation rate $g_n(\zeta)$ is a function of $\bar{u}(\zeta)$ but is *independent of the derivatives of* $\bar{u}$. Hence F_n is independent of the flow profile in $\zeta' > \zeta$ and it follows that if momentum diffusion is negligible in (2.11) then *there can be no downward propagation of influence* in the mean flow. This is not in accord with the explanation of the downward motion of shear zones in HL; nevertheless, it will be shown in the following sections that this observation does not preclude such downward phase propagation. It *does* mean that the mean flow evolution at any particular level is independent of what takes place above.

Note that this principle applies for upward propagating waves. If these waves are reflected, either at a high-level boundary or internally (corresponding to a breakdown in the WKB approximation), it becomes invalid.

3. Forcing by a single wave

Steady solutions to (2.9)–(2.11) for the case of forcing by a single internal wave have been discussed by Plumb (1975). Here the evolution of such flows is briefly considered. Eqs. (2.9)–(2.11) were integrated numerically (using standard centered differences to represent the space and time derivatives) with 80 grid points in $0 \leqslant \zeta \leqslant 4$. Imposed data were $F_1(0)=1$, $k_1=1$, $c_1=1$ and $\alpha=1$; the boundary conditions $\bar{u}(0)=0$, $\partial\bar{u}/\partial\zeta\ (4)=0$ were used and the initial state was one of no motion. (The upper boundary should ideally be located at infinity; otherwise, for consistency, a reflected wave component should be included. However, $\zeta=4$ is sufficiently high that such effects are negligible).

Results for $\Lambda=0.1$ are presented in Fig. 1. Initially, $\bar{u}=0$ and, from (2.9) and (2.10), $F_1=e^{-\zeta}$. As the flow evolves $|\bar{u}-c|$ decreases and the wave is attenuated more rapidly, until a steady state is eventually established where viscosity balances the wave-driven acceleration of the mean flow. At low levels, this state

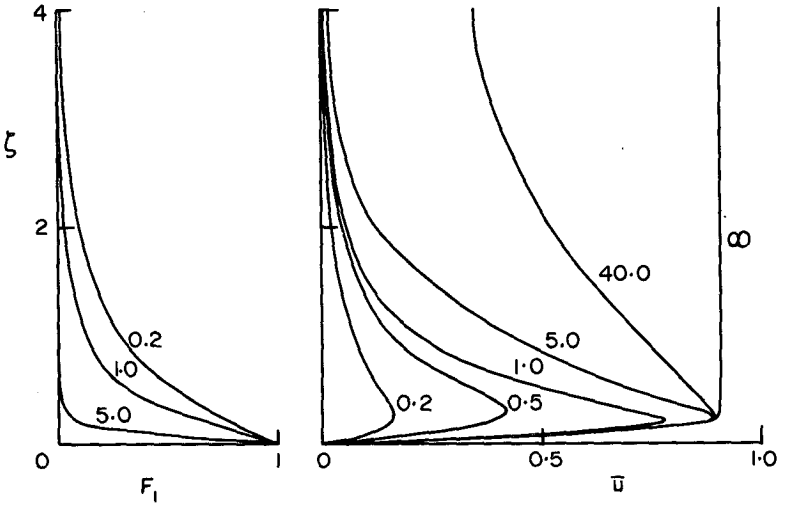

FIG. 1. Profiles of mean velocity $\bar{u}$ and wave momentum flux F for single-wave forcing with $\Lambda=0.1$. Curves are labeled with time τ.

Brought to you by New York University | Unauthenticated | Downloaded 10/07/21 07:05 PM UTC

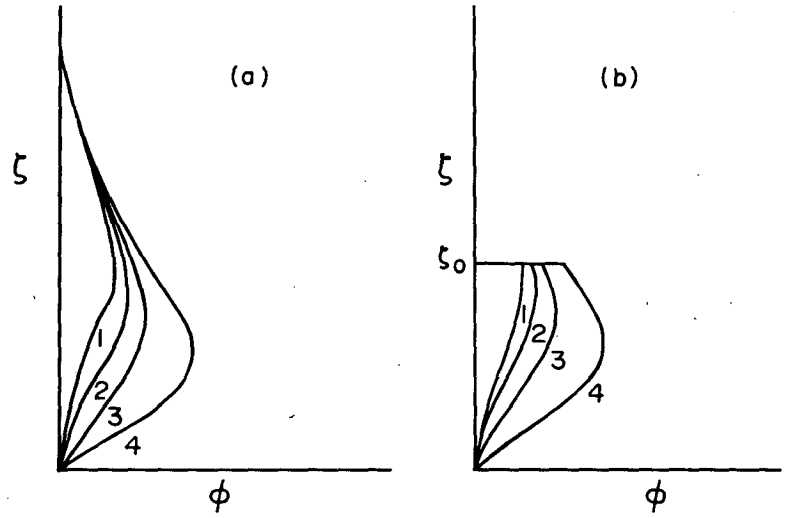

FIG. 2. Evolution of mean streamfunction ϕ in linear inviscid problem showing downward motion of the ϕ maximum (a); part (b) is identical below $\zeta=\zeta_0$.

is characterized by a strong shear, but at large ζ $\bar{u}\to(1+\Lambda)^{-1}$ (Plumb, 1975).

Other integrations with Λ as small as 0.005 showed similar behavior. In particular, a steady state was always ultimately established; the case of a single wave forcing apparently has a stable steady solution at least for $0.005\leqslant\Lambda\leqslant 1$.

4. Stability in the presence of two waves

If two upward propagating wave components are present it is in principle possible to obtain steady solutions as for the single wave case. However, as will be shown below, such solutions are unstable (at least for small viscosity) and hence of limited interest.

Consider the simplest problem of two waves, with $F_1(0)=-F_2(0)=0.5$, $k_1=k_2=1$ and $c_1=-c_2=1$, propagating through a uniform fluid with $\alpha=1$. The steady equilibrium solution to (2.9)–(2.11) is, trivially, $\bar{u}(\zeta)=0$ with $F_1(\zeta)+F_2(\zeta)=0$ everywhere. Perturbing this state such that

$$|\bar{u}|\ll 1, \quad \left|\int \bar{u}d\zeta'\right|\ll 1$$

everywhere, the linearized form of (2.9)–(2.11) becomes

$$\frac{\partial\bar{u}}{\partial\tau}-\Lambda\frac{\partial^2\bar{u}}{\partial\zeta^2}=2\left(\bar{u}-\int_0^\zeta \bar{u}d\zeta'\right)e^{-\zeta}. \tag{3.1}$$

The two terms on the right-hand side correspond to the two contributions to wave forcing discussed by HL. If $\bar{u}>0$, the wave of positive phase velocity is attenuated more rapidly, since $|\bar{u}-c_1|$ is decreased (and hence the vertical group velocity is reduced), in accordance with (2.10). Conversely, the negative wave is attenuated less, and there is thus a net positive mean flow acceleration. This amplification effect which is the basis for the instability is represented by the first term on the right-hand side of (3.1). The second "shielding" term describes the influence on the wave momentum fluxes at a given level of the integrated effect of absorption below, and is the dominant term at upper levels.

Defining the mean streamfunction

$$\phi(\zeta,\tau)=\int_0^\zeta \bar{u}(\zeta',\tau)d\zeta', \tag{3.2}$$

Eq. (3.1) becomes

$$\partial\phi/\partial\tau=2\phi e^{-\zeta}+\Lambda\left[\frac{\partial^2\phi}{\partial\zeta^2}(\zeta,\tau)-\frac{\partial^2\phi}{\partial\zeta^2}(0,\tau)\right]. \tag{3.3}$$

Clearly, if $\Lambda=0$ this equation has the solution

$$\phi(\zeta,\tau)=\phi(\zeta,0)\exp(2\tau e^{-\zeta}); \tag{3.4}$$

the flow is unstable, ϕ amplifying with a growth rate that decays with height.[4] This differential amplification leads to downward propagation of ϕ maxima (zeros of $\bar{u}$), as shown schematically in Fig. 2a. Note that this does not contradict the principle of no downward propagation of influence; Fig. 2b depicts the evolution from initial conditions identical with those of the first case below ζ_0, but $\phi=0$ in $\zeta>\zeta_0$. The subsequent development in $\zeta<\zeta_0$ is identical in the two cases.

[4] N.B. The factor $e^{-\zeta}$ is not merely a reflection of the same term in (3.1) which represents the unperturbed decay of the individual wave fluxes. It is also a consequence of the functional form of

$$\bar{u}-\int^\zeta \bar{u}d\zeta'=e^\zeta\frac{d}{d\zeta}\left[e^{-\zeta}\int^\zeta \bar{u}d\zeta'\right].$$

Brought to you by New York University | Unauthenticated | Downloaded 10/07/21 07:05 PM UTC

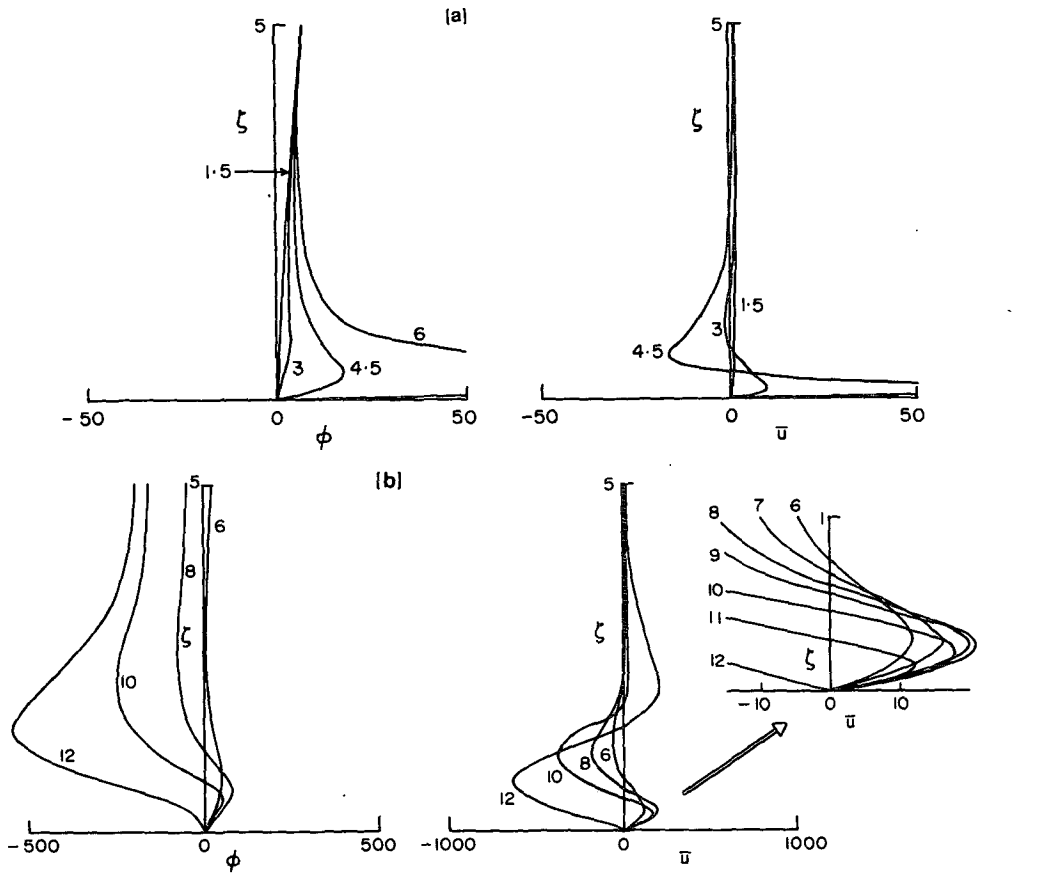

FIG. 3. Evolution of ϕ and $\bar{u}$ in linear problem from initial conditions $\bar{u}(\zeta,0)=\tanh(\zeta-1)-\tanh(1)$ for (a) $\Lambda=0$, (b) $\Lambda=0.04$. Inset shows detail below $\zeta=1$. Curves are labeled with time τ.

The evolution from initial conditions $\bar{u}(\zeta,0)=\tanh(\zeta-1)-\tanh(1)$ is shown in Fig. 3a. As amplification proceeds, a maximum in ϕ develops at $\tau\approx 3$ and $\zeta\approx 0.8$, so that, immediately above this level, $\bar{u}$ becomes negative. This region of negative flow grows in amplitude and extends in both directions; below the downward moving shear zone, the positive jet amplifies and becomes narrower with time. This behavior continues idefinitely. The underlying dynamics of the instability are essentially those discussed in HL. At low levels the local attenuation term in (3.1), $2\bar{u}e^{-\zeta}$, is the major contribution and the positive flow there is amplified. At large ζ, however, the shielding term $2e^{-\zeta}\int\bar{u}d\zeta'$ becomes dominant and the acceleration is negative even when $\bar{u}>0$. The change of sign occurs at ζ_0 where

$$\bar{u}(\zeta_0)=\int_0^{\zeta_0}\bar{u}d\zeta'. \tag{3.5}$$

Now, below ζ_0, $\partial\bar{u}/\partial\tau>0$. Hence the shielding term increases with time, while $\partial\bar{u}(\zeta_0)/\partial\tau=0$. Since $\partial\bar{u}(\zeta_0)/\partial\zeta<0$, ζ_0 must descend in order to preserve balance in (3.5). Thus the downward motion of the change of sign in wave forcing is, in accordance with arguments expressed above, in response to the flow evolution at lower levels.

Once a zero in $\bar{u}$ has been established, it follows from (3.1) that only the shielding term contributes to the forcing at the level of the zero. Hence the lowest zero of $\bar{u}$ moves downward irrespective of the time-dependence of the low level flow. Note that the upper zero of $\bar{u}$ moves upward; this is because the lowest (positive) flow zone is more effective as a barrier to the positive wave than the negative zone is to the negative wave. Hence the acceleration is negative and the zero moves upward.

With nonzero viscosity, diffusion of the narrowing jet at low levels has profound consequences for the flow evolution. Fig. 3b shows the results for $\Lambda=0.04$. The early evolution, $\tau<6$, is similar to the corresponding inviscid evolution except that the shears are much reduced. After $\tau\approx 6$, diffusion of the lowest (positive) jet becomes more significant, so that at $\tau\approx 8$, its growth is completely halted. Note that the negative jet, being much broader, continues to amplify and by the time $\tau=8$ the negative barrier is more effective than the positive one. The second zero of $\bar{u}$ then begins to

Brought to you by New York University | Unauthenticated | Downloaded 10/07/21 07:05 PM UTC

move downward as the acceleration at high levels becomes positive. After $\tau \approx 8$ diffusion begins to destroy the positive jet until, at $\tau \approx 12$, it has disappeared altogether. The process then repeats, the evolution being governed by essentially inviscid dynamics until the negative jet narrows and diffusion once again begins to take effect. Thus, as discussed by HL, the viscous "switching" produces an oscillatory solution.

The precise means by which diffusion destroys the lowest jet will subsequently be shown to be of some practical importance. Details of the flow evolution in $\zeta < 1$ and $6 \leqslant \tau \leqslant 12$ are shown in the inset to Fig. 3b. The role of diffusion is twofold. First, the region of positive shear becomes almost steady (in the same way as in the single wave flows); then the jet is destroyed from above by diffusive interaction with the advancing negative jet. Thus the most significant viscous effects occur in an interior shear layer and the presence of the momentum sink at the lower boundary may not be essential to the switching mechanism.

The characteristics of the linear system for various values of Λ are summarized in Table 1. The "growth rate" is evaluated at $\tau = 1$ by taking the values of ϕ as successive maxima (zeros of $\bar{u}$) pass through that level; good fits were obtained on a $\ln\phi$ vs τ plot in all cases. The vertical scale is the height of the first zero of $\bar{u}$ at the time when $\partial\bar{u}(0,\tau)/\partial\zeta$ changes sign. Remarkably, the oscillation period is (for $\Lambda \neq 0$) almost independent of Λ; the case $\Lambda = 0$ appears to be singular. The growth rate decreases smoothly from a value of 0.738 at $\Lambda = 0$ to zero at $\Lambda = 0.112$ (the time-decaying solution found at $\Lambda = 0.12$ still exhibits oscillatory behavior). It may seem surprising that such a small viscosity can inhibit the instability. However, in the interior shear layer the main coutribution to the wave forcing is the shielding term; this becomes comparable with the viscous term when the height scale of the shear layer is $O(\Lambda^{\frac{1}{3}})$. At the stability transition $\Lambda^{\frac{1}{3}} = 0.48$ and the effects of viscosity are significant over a depth of fluid not much smaller than the height scale (unity) of the forcing. This interpretation was endorsed by a comparison of terms in (3.1) in the case $\Lambda = 0.10$.

TABLE 1. Characteristics of the linearized two-wave problem.

Λ	Growth rate	Period	Vertical scale
0.0	0.738	—	—
0.02	0.724	19	1.0
0.04	0.429	19	1.5
0.06	0.260	20	2.0
0.08	0.142	20	2.4
0.10	0.049	20	3*
0.12	−0.013	21	3*

* Values change with time.

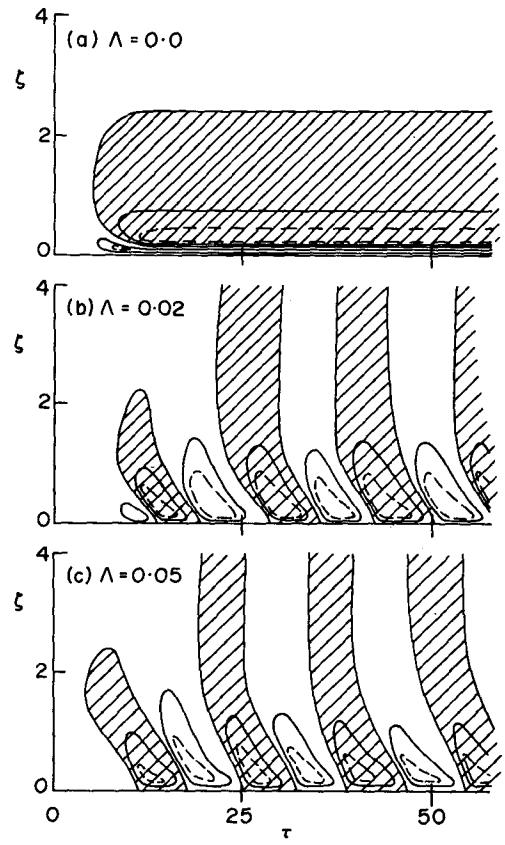

FIG. 4. Results of nonlinear integration of (2.9)–(2.11) for $\alpha = 1$, $F_1 = 0.5$, $k_1 = 1$, $c_1 = 1$, $F_2 = -0.5$, $k_2 = 1$, $c_2 = -1$. Contours of mean zonal velocity $\bar{u}$ are shown on a time-height plot. Regions of negative $\bar{u}$ are shaded. Solid lines are at intervals of 0.5; dashed contours represent ± 0.75. See text for elaboration.

5. The nonlinear flow

Fully nonlinear solutions (subject to the WKB approximation) appropriate to the standing-wave forcing discussed in the previous section were determined by numerical integration of (2.9)–(2.11) with $F_1(0) = -F_2(0) = 0.5$, $k_1 = k_2 = 1$, $c_1 = -c_2 = 1$ and $\alpha = 1$. The finite-difference grid consisted of 80 points in $0 \leqslant \zeta \leqslant 4$; boundary conditions were $\bar{u}(0) = 0$, $\partial\bar{u}/\partial\zeta(4) = 0$. Results of integration from the initial condition

$$\left.\begin{aligned} \bar{u}(\zeta,0) &= 0.03\zeta, \quad \zeta \leqslant 3.333 \\ \bar{u}(\zeta,0) &= 0.1 \quad\;\; , \quad \zeta > 3.333 \end{aligned}\right\}$$

are shown in Fig. 4. The inviscid flow (Fig. 4a) is qualitatively similar to the corresponding linear solution, the main difference being that $|\bar{u}|$ never exceeds a value of 1, i.e., no critical levels are established. Forcing by internal waves cannot generate a critical level if none exists originally[5] (Plumb, 1975) and a limit is thus imposed on the flow speeds. The positive

[5] This remark depends on the WKB approximation and the assumption of mean flow steadiness.

Brought to you by New York University | Unauthenticated | Downloaded 10/07/21 07:05 PM UTC

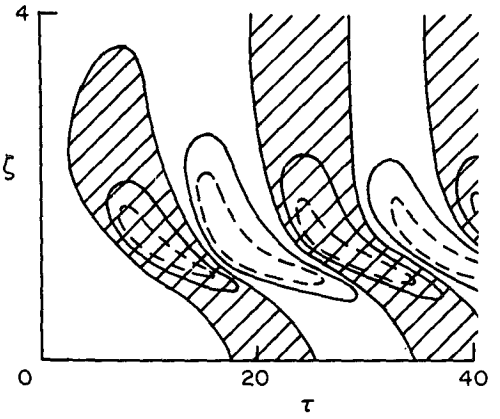

FIG. 5. As in Fig. 4, with $\Lambda=0.02$, except for

$$\alpha=\begin{cases}0, & \zeta<1,\\ \cos^2\{\pi(\zeta-1.5)\}, & 1\leqslant\zeta\leqslant 1.5\\ 1 & \zeta\geqslant 1.5\end{cases}$$

and negative flow maxima do approach $\bar{u}=\pm 1$ asymptotically in this inviscid case. Another difference is that the flow at the highest levels remains positive. This is a result of the enhanced shielding in the nonlinear problem [which becomes total as $\bar{u}\to\pm 1$; see (2.10)]; thus the wave driving is so weakened above the two jets (the wave fluxes are reduced by a factor of about 10^{-6} across their respective barriers at $\tau=25$) that acceleration at high levels is negligible. With nonzero viscosity (Figs. 4b, 4c), the oscillatory behavior is evident. After a transient phase ($\tau\lesssim 25$,[6] depending on Λ) the motion settles down to a regular oscillation which was found to be independent of the initial conditions. The maximum flow speeds are ± 0.96 with $\Lambda=0.02$ and ± 0.85 for $\Lambda=0.05$. The period is again almost independent of Λ. Its value (≈ 14.0) is rather less than in the linear problem; this decrease is a result of the increased shielding. For example, during the positive flow phase at low levels the positive wave component is, for practical purposes, completely absorbed while the negative wave suffers little attenuation. Thus the fluid at high levels experiences strong negative acceleration and the time scale is reduced.

Note how the flow at the lowest levels remains steady during a large part of each half-cycle, as in the linear flow. In order to illustrate the role of interior, rather than boundary, dissipation in destroying the lowest jet, the integration with $\Lambda=0.02$ was performed with

$$\alpha=\begin{cases}0, & \zeta<1\\ \cos^2[\pi(\zeta-1.5)], & 1\leqslant\zeta<1.5\\ 1, & \zeta\geqslant 1.5.\end{cases}$$

Thus below $\zeta=1$, the fluid is completely transparent to the waves and experiences no wave driving. Results are shown in Fig. 5. Exchange of momentum with the lower boundary is now insignificant and the switching from one regime to another is clearly a consequence of diffusion across the internal shear layer which develops at $\zeta\approx 1$, i.e., at the lowest level where the effects of wave driving appear. Thus diffusive switching may be relevant to the atmospheric case[7] (where boundary effects cannot be important).

[6] Adjustment is considerably slower at the higher levels.

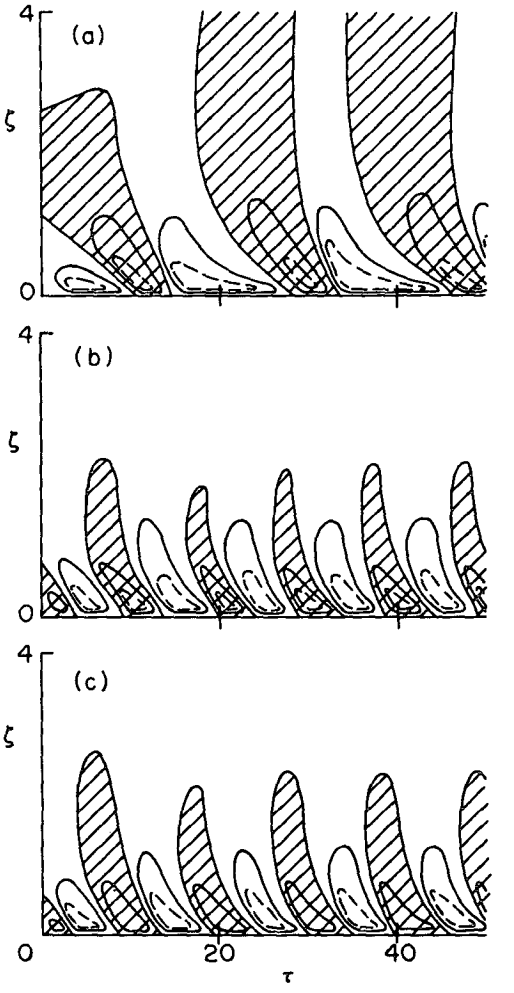

FIG. 6. As in Fig. 4, except for (a) $F_1=0.67$, $F_2=0.33$, $\Lambda=0.04$; (b) $k_2=0.5$, $\Lambda=0.02$; (c) $c_2=-0.75$, $\Lambda=0.02$.

6. Generalizations

Results of integration for less specific cases (in which the two wave components are not simply equal and opposite) are presented in Fig. 6. In each case the flow was initialized with $\bar{u}(\zeta,0)=0$.

[7] HL speculated that this might be so, but on the grounds that, in reality, the shear layers would become sharp enough to be unstable. However, it was suggested by Plumb (1975) that as $\mathrm{Ri}\to\frac{1}{4}$, the momentum fluxes may vanish (see also Ramanathan and Cess, 1975); if so, unstable mean shear layers cannot be generated by this mechanism.

Brought to you by New York University | Unauthenticated | Downloaded 10/07/21 07:05 PM UTC

The consequences of unequal momentum fluxes are shown in Fig. 6a for which $F_1(0)/F_2(0)=-2$. The asymmetry of the oscillation is clear. The positive flow regime moves downward at a faster rate (i.e., positive accelerations are of larger magnitude) and with a stronger associated shear than the negative regime. Consequently, the positive jet near the lower boundary is longer lived than the negative jet; as a result of shielding at low levels, the opposite asymmetry obtains at higher levels.

A flow driven by two waves of different wavenumber is shown in Fig. 6b, where $F_1(0)=-F_2(0)$ but $k_1/k_2=2$. For present purposes, the only important consequence of the unequal wavenumbers is unequal vertical penetration of the two waves, the respective momentum fluxes varying as $e^{-\zeta}$ and $e^{-2\zeta}$ when $\bar{u}=0$. It follows that the flux divergence is dominated by the negative wave ($i=2$) at low levels, and by wave 1 at large ζ. This is clearly apparent in Fig. 6b where negative accelerations are the larger below $\zeta\approx 1$ while the flow is always positive above $\zeta\approx 2$.

Two separate effects are found when the phase speeds of the two waves differ in magnitude. The first is the same as in the previous example; the vertical penetration depths are unequal. More directly, the nonlinear limit that $\bar{u}$ can never exceed either phase speed (i.e., with $c_1>0$, $c_2<0$, then $c_2<\bar{u}<c_1$) means that the flow maxima are correspondingly restricted. Both these effects are apparent in Fig. 6c, for which $c_1=1$ while $c_2=-0.75$. The vertical structure is similar to that in Fig. 6b; the flow maxima are asymmetrical as anticipated, being 0.95 and -0.72.

Clearly, the instability discussed in Section 4 obtains in situations more general than the simple case presented therein, and the basic properties of the mean flow evolution remain qualitatively unchanged. Those differences of detail that do occur have simple explanations in terms of the structure of the imposed waves. With regard to the different dimensionless periods evident in Fig. 6, it should be noted that in these asymmetrical cases there is no unique choice of the scaling factors on which the definition of the dimensionless variables is based.

7. Solutions in an atmosphere

The discussion so far has been restricted to Boussinesq fluids with uniform mean density. In the atmosphere such an approximation is not appropriate; while compressibility is unimportant in the local dynamics, the concomitant decay of mean density with height can have profound effects on the vertical structure of the mean motion. Therefore, following Lindzen (1971), the Boussinesq approximation is adopted locally while the mean density is a function of ζ, when (2.11) becomes

$$\frac{\partial \bar{u}}{\partial \tau}-\Lambda\frac{\partial^2 \bar{u}}{\partial \zeta^2}=-\frac{\bar{\rho}(0)}{\bar{\rho}(\zeta)}\sum_n \frac{\partial F_n}{\partial \zeta}; \tag{7.1}$$

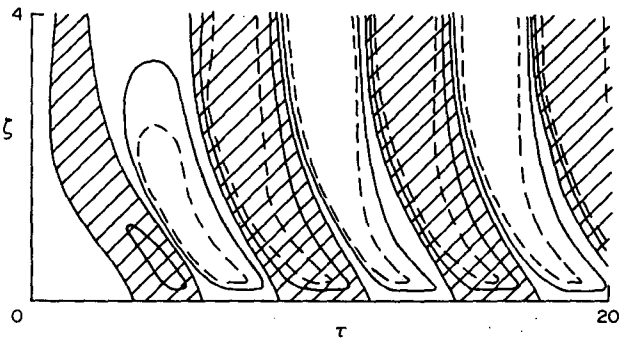

FIG. 7. As in Fig. 4, except in an atmosphere with $\epsilon=1$.

Eqs. (2.9) and (2.10) are unchanged. In an isothermal atmosphere $\bar{\rho}(Z)=\bar{\rho}(0)e^{-z/H}$ (where H is a constant) or, in terms of the dimensionless coordinate, $\bar{\rho}(\zeta)=\bar{\rho}(0)e^{-\epsilon\zeta}$ where $\epsilon=h/H$ and h is the height scale defined in (2.8). Then (7.1) becomes

$$\frac{\partial \bar{u}}{\partial \tau}-\Lambda\frac{\partial^2 \bar{u}}{\partial \zeta^2}=-e^{\epsilon\zeta}\sum_n \frac{\partial F_n}{\partial \zeta}. \tag{7.2}$$

The examples considered so far correspond to the limit $\epsilon\to 0$. The effect of nonzero ϵ is clearly, from (7.2), to increase the acceleration at high levels and in consequence the vertical scale of the oscillation is increased. Indeed, when $\epsilon=1$, the $e^{-\zeta}$ decay of the momentum fluxes in the linear problem is counteracted[8] by this density factor in (7.2) and the flow, at high levels, becomes independent of height. This, as shown in Fig. 7, is reflected in the full nonlinear motion. Note that if $\epsilon>1$, this argument suggests a tendency for the amplitude of the oscillation to increase with height. However, this is not apparent in calculations performed with $\epsilon>1$ because the amplitude reaches its limit (close to unity) at low levels and cannot exceed this value above.

A significant consequence of the enhanced wave-driving is that the effective magnitude of viscous effects relative to this forcing is reduced at high levels. This manifests itself in two ways. The period of the oscillation is governed by the time required for the interior shear layer to become narrow enough for diffusion to become significant and thereby to dissipate the low-level jet. For small viscosity ($\Lambda\lesssim 0.02$) the interior shear layer is located at small ζ where the effects of finite ϵ are small, and the period is close to that (~ 14) found for $\epsilon\to 0$. However, as Λ increases the shear layer extends to higher levels where the acceleration is more rapid than in the case $\epsilon=0$ and so the period decreases. For example, when $\epsilon=0.05$, the period is about 7.5, while

[8] Note that this does not negate the discussion of the origins of downward phase propagation in Section 3. The shielding term still fulfills the same role as in the case $\epsilon=0$.

Brought to you by New York University | Unauthenticated | Downloaded 10/07/21 07:05 PM UTC

TABLE 2. Scaling factors for the HL model.

$\hat{c}$	30 m s^{-1}
$\hat{k}$	1.57×10^{-7} m^{-1}
$\hat{F}$	8.0×10^{-3} m^2 s^{-2}
$\hat{\alpha}$	10^{-6} s^{-1}
$\hat{N}$	2.16×10^{-2} s^{-1}

if $\Lambda=0.1$ (Fig. 7) it is about 5.0.[9] Second (and for the same reasons) the transition to stability takes place at higher Λ—it was noted earlier that this transition occurs when diffusion becomes important throughout the interior where, if $\epsilon>0$, the effective viscosity decreases. With $\epsilon=1$, it was found that the flow decayed if $\Lambda\gtrsim0.4$.

8. The Holton-Lindzen model

As a simulation of the dynamics of the tropical stratosphere the model described in HL is considerably more realistic than the examples presented above; the HL model is a two-dimensional one (thus ignoring Coriolis effects), although the functional forms of the wave momentum fluxes are those appropriate to fully three-dimensional waves on an equatorial β plane. From Lindzen (1971) the attenuation rates are, in the notation of Section 2,

$$\left.\begin{aligned} g_1&=\frac{\alpha}{k_1(\bar{u}-c_1)^2}\quad\text{(Kelvin wave)}\\ g_2&=\frac{\alpha}{k_2(\bar{u}-c_2)^2}\left[\frac{\beta'}{k_2^2(\bar{u}-c_2)}-1\right]\\ &\qquad\qquad\text{(Rossby-gravity wave)}\end{aligned}\right\},\quad(8.1)$$

where $\beta'=\beta/\hat{k}^2\hat{c}$, β being the usual (equatorial) beta parameter. Only these two waves are considered.

This approach is not without pitfalls (Andrews and McIntyre, 1976a,b); the HL model is used here as a vehicle for assessing the consequences of the foregoing calculations to the existing theory. The reader is referred to HL for full details of the data used; the scaling factors appropriate to the present notation are listed in Table 2. In dimensionless terms, $F_1(0)=-F_2(0)=0.5$, $k_1=1$, $k_2=4$ and $c_1=-c_2=1$ (note that westerly motion is positive). The vertical scale is 6.62 km; an isothermal atmosphere with $H=6$ km corresponds to $\epsilon=1.1$. The dissipation profile is

$$\alpha=\begin{cases}0.55+0.56\zeta, & \zeta\leqslant1.97\\ 1.65, & \zeta>1.97\end{cases}$$

where $\zeta=0$ represents the level $z=17$ km above ground. Unit dimensionless time corresponds to 285 days and for $\nu=0.3$ m^2 s^{-1}, $\Lambda=0.17$; the beta parameter $\beta'=30.8$.

[9] Similarly, for fixed Λ, the period decreases with increasing ϵ.

The problem is defined by (2.9), (8.1) and (7.2); these equations were integrated numerically in $0\leqslant\zeta<2.72$ with 78 grid points therein and with $\bar{u}(0)=0$ and $\partial\bar{u}/\partial\tau(2.72)=0$. The upper boundary is undesirably low—the Rossby-gravity wave flux decays only by about half its maximum value over this depth when $\bar{u}=0$. However, in view of the lack of downward influence, unphysical effects should be contained near the upper boundary.

Fig. 8a shows the results of such a calculation with, following HL, an additional forcing term on the right-hand side of (7.2)

$$G(\zeta,\tau)=\begin{cases}0, & \zeta\leqslant1.66\\ 4.37(\zeta-1.66)\sin(9.76\tau), & \zeta>1.66\end{cases}$$

to simulate the "semi-annual" oscillation at high levels. This feature is obvious above $\zeta\approx2$ but at lower levels the longer period wave-driven oscillation is dominant. The figure should be compared with Fig. 1 of HL; in the main the differences are small except that the period found here is close to three years rather than the value of 26.5 months reported by HL.

The results of the calculation without semi-annual forcing are given in Fig. 8b. The similarity with Fig. 8a is clear (of course, the high-level forced oscillation has disappeared) in agreement with the principle that, if $\Lambda=0$, anomalies introduced at high level do not influence the motion below. Since Λ is nonzero, some small changes have occurred; for example, the period is reduced by a factor of 0.08 (a similar comparison at $\Lambda=0.05$ produced a fractional change of 0.02). The structure of the oscillation is asymmetrical as a result of the different attenuation rates of the two waves. For the Kelvin wave, $g_1(\zeta)$ varies from 0.55 to 1.65 between $\zeta=0$ and $\zeta=2.72$, while the corresponding values for $g_2(\zeta)$ are 0.13 and 0.39. Hence $g_2(\zeta)<\epsilon$ at all levels and, from the arguments of Section 7, the amplitude of the easterly phase should be independent of height at high levels. For the Kelvin wave $g_1(\zeta)<\epsilon$ below $\zeta=0.8$ but $g_1(\zeta)>\epsilon$ above so that the westerly phase should decay with height above that level. These features are apparent in Fig. 8b; the strong easterly accelerations at high levels are probably similarly due to the greater penetration of the easterly wave.

The second variation presented here is the adoption of a height-independent cooling coefficient (HL report such a calculation in a footnote). The results with $\alpha=1$ are presented in Fig. 8c. With $\alpha=1$, $g_1=1$ and $g_2=0.23$ at all heights and hence the vertical structure of both easterly and westerly phases of the oscillation becomes almost independent of height at high levels. However, the most striking difference between Figs. 8b and 8c is in the temporal structure—the westerly regime is almost three times more long-lived than the easterly. The explanation of this phenomenon seems to

Brought to you by New York University | Unauthenticated | Downloaded 10/07/21 07:05 PM UTC

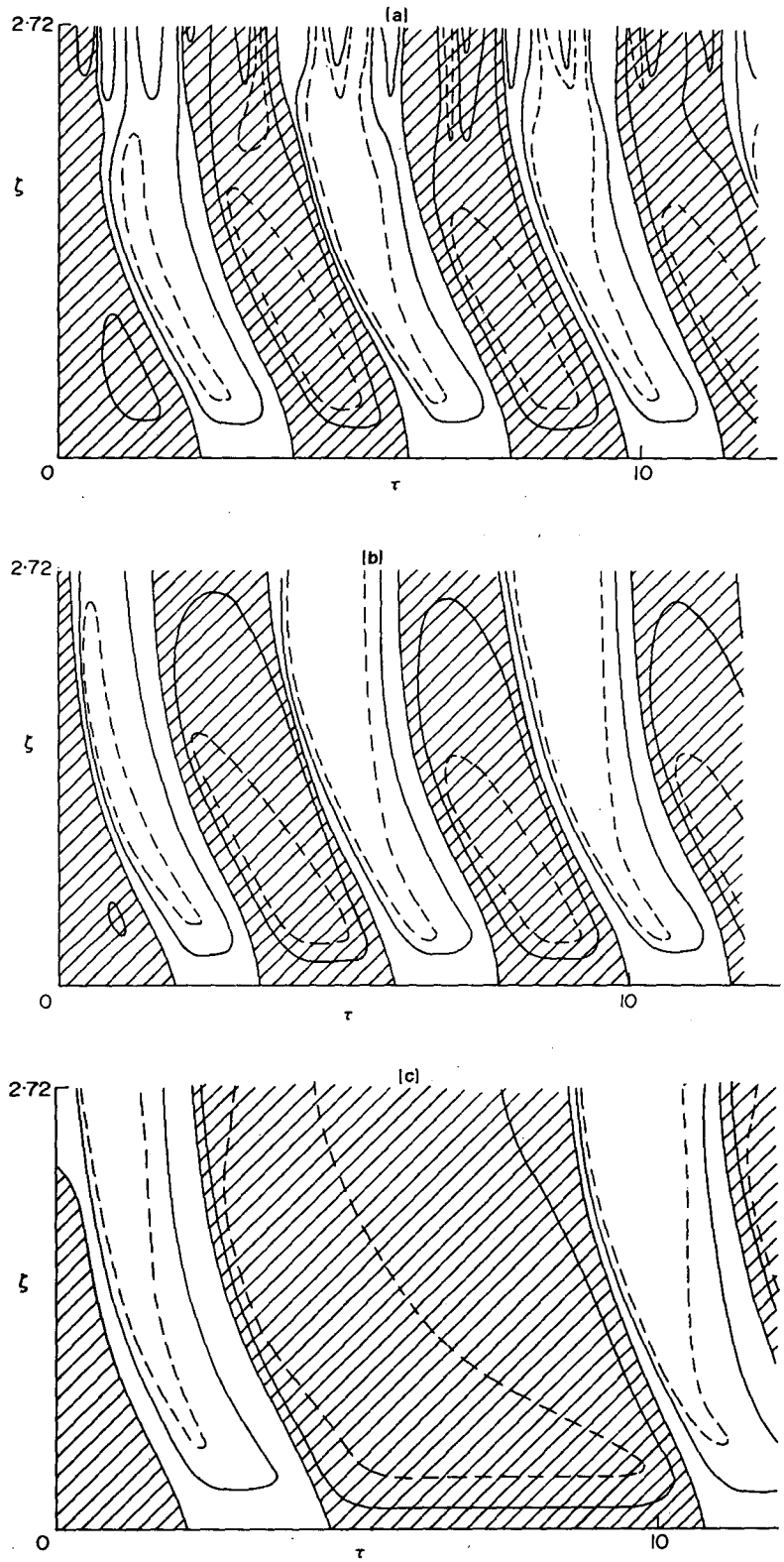

FIG. 8. Zonal flow contours for models of the equatorial stratosphere: (a) HL model, described in text; (b) HL model without semi-annual forcing; (c) as in (b) but with uniform dissipation, $\alpha=1$. Westerlies are shaded, otherwise the contouring convention is as Fig. 4.

Brought to you by New York University | Unauthenticated | Downloaded 10/07/21 07:05 PM UTC

be as follows. Associated with the increased penetration of the westerly phase, the maximum westerly flow speed is increased (to 0.90 as against 0.78 in Fig. 8b). Now, the attenuation rate $g_2(\zeta)$ contains the factor

$$\frac{\beta'}{k_2^2(\bar{u}-c_2)}-1$$

which vanishes[10] when $\bar{u}-c_2=1.92$, i.e., $\bar{u}=0.92$. Therefore when $\bar{u}$ approaches 0.92, $g_2(\zeta)$, and hence the easterly acceleration also, becomes very small. Therefore the westerly regime is removed very slowly; the situation is compounded by the effects of smaller α at high levels which also reduces the easterly acceleration.

This sensitivity arises from the fact that $g_2(\zeta)$ has a zero when the mean flow velocity is between its limiting values $c_1>\bar{u}>c_2$, i.e., the quantity $b=\beta/k_2^2(c_1-c_2)$ [dimensional quantities] is less than unity. With the given data, $b=0.96$. However, according to Maruyama (1967) $c_2=-23$ m s^{-1} and $b=1.09$; the data of Lindzen and Tsay (1975) for the Rossby-gravity wave given $k_2=4.72\times10^{-7}$ m^{-1} and $c_2\approx-35$ m s^{-1}, whence $b=1.58$. Hence this sensitivity may be much reduced if more realistic data were used.

9. Discussion

From this study of the stability and evolution of the mean flow in the presence of two internal waves the essential characteristics of the mean-flow oscillation were shown to be basically as described by the Holton-Lindzen theory of the quasi-biennial oscillation, but with two significant modifications. First, the downward phase propagation should be interpreted with caution. This phenomenon is a consequence of the flow evolution at lower levels only and it is conceptually incorrect to regard the successive flow regimes as being initiated from above. Thus it was shown that it is not essential to the basic mechanism that the cooling coefficient increase with height, while the semi-annual oscillation at high levels in the tropical atmosphere has little relevance for the quasi-biennial oscillation below. The second significant result is the clarification of the role of viscosity. Without dissipation of the lowest jet the flow attains an almost steady state. The dissipation is principally achieved not by momentum exchange with the lower boundary (which only serves to maintain a quasi-steady flow at certain phases of the oscillation) but by diffusion across the internal shear layer which separates the lowest jet from the oppositely directed flow immediately above. This diffusive switching may therefore be relevant in the real atmospheric case. Otherwise, the switching would have to occur via interaction of the mean flow with the wave generation process. If, as believed, the waves concerned are generated in the troposphere, this seems unlikely since the amplitude of the zonal wind oscillation decreases rapidly below about 20 km (Wallace, 1973).

The dependence of the period and other characteristics of the oscillation on the imposed parameters have been elucidated in some simple cases. The period is given by

$$T=\eta\frac{\hat{k}\hat{c}^3}{\hat{N}\hat{\mu}\hat{F}},$$

where η is a dimensionless number which depends on the precise details of the problem. In the case of symmetrical forcing (the only one where definition of the scaling factors is unambiguous) $\eta\approx14$ in a Boussinesq fluid but it decreases rapidly with increasing ϵ in a compressible atmosphere. The vertical structure also varies with ϵ. When $\epsilon=0$, successive flow regimes first appear at $\zeta\approx1$ and penetrate little above this level. The vertical scale increases with ϵ until $\epsilon\gtrsim1$ when the regimes appear almost simultaneously at all heights $\zeta\gtrsim2$ and the structure is almost independent of height at these levels. This is apparently the case in the tropical stratosphere, where the oscillation amplitude is almost constant above 25 km (Wallace, 1973).

The basic parameters will, in reality, vary with time. Short-period changes should not have much effect but any slower changes in the climate of the equatorial troposphere (affecting the generation mechanism and hence F and perhaps k and c) or in the stratosphere (affecting N and μ) would be reflected in long-term changes in the period (and other characteristics) of the zonal wind oscillation. Hence changes in the oscillation period such as that which apparently occurred around 1962 (McInturff and Miller, 1972) are not inconsistent with the theory.

In principle, the calculations discussed here can be extended to include more than two forcing waves. There is evidence that at least three waves play a significant role in the stratosphere. Lindzen and Tsay (1975) showed that in addition to the two considered by HL, an easterly Rossby wave makes a significant contribution, particularly at high levels. They calculated the mean acceleration due to these three waves and found good agreement with the observed acceleration above 23 km, but a large deficit in the momentum budget remained below that level. They suggested that the required forcing could be provided by an easterly gravity wave of unit zonal wavenumber. However, Andrews and McIntyre (1976b) argued that this could not make up for the observed shortfall away from the equator and instead suggested that long-period Rossby waves might be responsible for the easterly acceleration below 23 km.

The present work leads to an alternative postulate in which there may be no need for additional wave driving.

[10] This is associated with a singularity in the meridional structure of the Rossby-gravity wave (see Lindzen, 1971).

Brought to you by New York University | Unauthenticated | Downloaded 10/07/21 07:05 PM UTC

If diffusion is indeed the basic switching mechanism, then, below the level of maximum amplitude of the wind oscillation ($\sim$23 km), momentum diffusion must be considered *a priori* on an equal footing with wave forcing. Inspection of Lindzen and Tsay's mean velocity profile (their Fig. 1) gives a typical value of $\partial^2\bar{u}/\partial z^2 \approx 5\times10^{-6}$ m^{-1} s^{-1} between 20 and 23 km. With $\nu = 0.3$ m^2 s^{-1} [11] the diffusive contribution gives an easterly acceleration of $\sim 1.5\times10^{-6}$ m s^{-2}; this is about one-half of the deficit found by Lindzen and Tsay. Thus it is clear that diffusive fluxes are important in this region. Given the crudity of this calculation it is possible that the divergence of the diffusive flux represents the major contribution to $\partial\bar{u}/\partial t$ below 23 km.

Acknowledgments. I am grateful to Drs. D. G. Andrews, M. E. McIntyre and P. J. Webster and to an anonymous referee for constructive comments on an earlier version of this paper.

REFERENCES

Andrews, D. G., and M. E. McIntyre, 1976a: Planetary waves in horizontal and vertical shear: The generalized Eliassen-Palm relation and the mean zonal acceleration. *J. Atmos. Sci.*, **33**, 2031–2048.

——, and ——, 1976b: Planetary waves in horizontal and vertical shear: Asymptotic theory for equatorial waves in weak shear. *J. Atmos. Sci.*, **33**, 2049–2053.

Boyd, J., 1976: The noninteraction of waves with the zonally-averaged flow on a spherical earth and the interrelationships of eddy fluxes of energy, heat and momentum. *J. Atmos. Sci.*, **33**, 2285–2291.

Fels, S. B., and R. S. Lindzen, 1974: The interaction of thermally excited gravity waves with mean flows. *Geophys. Fluid Dyn.*, **6**, 149–191.

Herring, J. R., 1963: Investigation of problems in thermal convection. *J. Atmos. Sci.*, **20**, 325–338.

Holton, J. R., and R. S. Lindzen, 1972: An updated theory for the quasi-biennial oscillation of the tropical stratosphere. *J. Atmos. Sci.*, **29**, 1076–1080.

Lindzen, R. S., 1971: Equatorial planetary waves in shear. Part I. *J. Atmos. Sci.*, **28**, 609–622.

——, and C. Y. Tsay, 1975: Wave structure of the tropical stratosphere over the Marshall Islands area during 1 April–1 July 1958. *J. Atmos. Sci.*, **32**, 2008–2021.

Maruyama, T., 1967: Large-scale disturbances of the equatorial lower stratosphere. *J. Meteor. Soc. Japan*, **45**, 391–408.

McInturff, R. M., and A. J. Miller, 1972: Note on variations in the quasi-biennial oscillation. *Mon. Wea. Rev.*, **100**, 785–787.

Newell, R. E., J. W. Kidson, D. G. Vincent, and G. J. Boer, 1974: *The General Circulation of the Tropical Atmosphere*, Vol. 2. The MIT Press, 371 pp.

Plumb, R. A., 1975: Momentum transport by the thermal tide in the stratosphere of Venus. *Quart. J. Roy. Meteor. Soc.*, **101**, 763–776.

Ramanathan, V., and R. D. Cess, 1975: An analysis of the strong zonal circulation within the stratosphere of Venus. *Icarus*, **25**, 89–103.

Wallace, J. W., 1973: General circulation of the tropical lower stratosphere. *Rev. Geophys. Space Phys.*, **11**, 191–222.

Wallace, J. W., and V. E. Kousky, 1968: On the relation between Kelvin waves and the quasi-biennial oscillation. *J. Meteor. Soc. Japan*, **47**, 496–502.

[11] Newell *et al.* (1974), commenting on the HL model, argue that this is three times larger than the value commonly accepted as being typical of the stratosphere. However, diffusion acts principally in the vicinity of strong shear zones where such a value is probably not unreasonably high. Indeed, if Ri is small enough in these shear zones, the waves may break where the *total* Richardson number (due to the waves and mean flow) decreases below 0.25, thus generating turbulent mixing of the intensity suggested by this interpretation.

Brought to you by New York University | Unauthenticated | Downloaded 10/07/21 07:05 PM UTC